

# Journal Pre-proof

Getting to and away from the egg, an interplay between several sperm transport mechanisms and a complex oviduct physiology

Laura Cecilia Giojalas, Héctor Alejandro Guidobaldi



PII: S0303-7207(20)30254-9

DOI: <https://doi.org/10.1016/j.mce.2020.110954>

Reference: MCE 110954

To appear in: *Molecular and Cellular Endocrinology*

Received Date: 9 March 2020

Revised Date: 3 July 2020

Accepted Date: 20 July 2020

Please cite this article as: Giojalas, L.C., Guidobaldi, Hé.Alejandro., Getting to and away from the egg, an interplay between several sperm transport mechanisms and a complex oviduct physiology, *Molecular and Cellular Endocrinology* (2020), doi: <https://doi.org/10.1016/j.mce.2020.110954>.

This is a PDF file of an article that has undergone enhancements after acceptance, such as the addition of a cover page and metadata, and formatting for readability, but it is not yet the definitive version of record. This version will undergo additional copyediting, typesetting and review before it is published in its final form, but we are providing this version to give early visibility of the article. Please note that, during the production process, errors may be discovered which could affect the content, and all legal disclaimers that apply to the journal pertain.

© 2020 Published by Elsevier B.V.

1 Getting to and away from the egg, an interplay between several sperm transport  
2 mechanisms and a complex oviduct physiology

3

4 Laura Cecilia Giojalas<sup>1</sup> and Héctor Alejandro Guidobaldi

5 Centro de Biología Celular y Molecular (FCEFYN- UNC), and Instituto de

6 Investigaciones Biológicas y Tecnológicas (CONICET – UNC), Córdoba, Argentina

7 <sup>1</sup> Corresponding author: lgiojalas@unc.edu.ar

8

### 9 **Abstract**

10 In mammals, the architecture and physiology of the oviduct are very complex, and  
11 one long-lasting intriguing question is how spermatozoa are transported from the  
12 sperm reservoir in the isthmus to the oocyte surface. In recent decades, several  
13 studies have improved knowledge of the factors affecting oviduct fluid movement  
14 and sperm transport. They report sperm-guiding mechanisms that move the  
15 spermatozoa towards (rheotaxis, thertotaxis, and chemotaxis) or away from the  
16 egg surface (chemorepulsion), but only a few provide evidence of their occurrence  
17 *in vivo*. This gives rise to several questions: how and when do the sperm transport  
18 mechanisms operate inside such an active oviduct? why are there so many sperm  
19 guidance processes? is one dominant over the others, or do they cooperate to  
20 optimise the success of fertilisation? Assuming that sperm guidance evolved  
21 alongside oviduct physiology, in this review we propose a theoretical model that  
22 integrates oviduct complexity in space and time with the sperm-orienting  
23 mechanisms. In addition, since all of the sperm-guidance processes recruit  
24 spermatozoa in a better physiological condition than those not selected, they could

25 potentially be incorporated into assisted reproductive technology (ART) to improve  
26 fertility treatment and/or to develop innovative contraceptive methods. All these  
27 issues are discussed in this review.

28

29 **Keywords:** sperm transport – oviduct peristalsis – rheotaxis – thermotaxis –  
30 chemotaxis

31

### 32 **1. Is there a need for sperm transportation to the egg?**

33 The mammalian spermatozoon is a small (around 60  $\mu\text{m}$  long in humans), highly  
34 differentiated cell with an optimised hydrodynamic shape, which carries only the  
35 organelles it will need to reach and fertilise the egg. For instance, it has an  
36 acrosome Golgi-derived vesicle to facilitate penetrating the egg vestments, a highly  
37 compacted DNA, and a long flagellum with a mitochondria network that generates  
38 the ATP necessary to propel it (Eddy, 2006). It might seem that, with the minuscule  
39 cargo it carries, its auto-propulsion would be enough to find the egg. But, is it?  
40 Apparently not. Even though the spermatozoon can swim some tens of  
41 micrometres per second, the distance it has to cover through the complex and very  
42 active female reproductive tract is several times its size (Boyd et al., 2018). Its own  
43 movement is evidently not enough to reach the egg. For instance, in the case of  
44 humans (Suarez and Pacey, 2006), semen is deposited at the bottom of the  
45 vagina, and from there the spermatozoa must first pass through the uterine cervix  
46 (around 4 cm long). This is a very complex structure with crypts and folds leading  
47 to the uterine cavity. The mucus filling the cervix is less dense at the bottom of the  
48 channels and this means that sperm is transported more easily along these than

49 through the central lumen, where strong fluid currents towards the vagina hinder  
50 the entrance of microorganisms. Once in the uterus, spermatozoa must cross a  
51 long distance (around 7 cm in humans) to get to the oviduct entrance, but this is  
52 facilitated by the peristalsis of the uterine muscle. Hence spermatozoa pass  
53 through the uterus very fast without major complications. Then, they must go  
54 through the uterus-tubal junction, which is a simple anatomical structure in humans  
55 and of variable complexity in other species (Harper et al., 1982; Suarez and Pacey,  
56 2006).

57 Once inside the oviduct, spermatozoa attach to the isthmus epithelium where they  
58 are physiologically prepared. It should be noted that spermatozoa coexist in  
59 different physiological states, and it is preferably the capacitated sperm  
60 subpopulation that reach and fertilise the egg (Cohen-Dayag et al., 1995; Oren-  
61 Benaroya et al., 2007; Uñates et al., 2014). Once spermatozoa complete  
62 capacitation, they detach from the epithelium, but there is still a long labyrinthine  
63 road (around 7 cm in humans and 25 cm in cows) to the fertilisation site, which is  
64 full of crypts and folds masking the egg's position (Burkitt et al., 2011; Yániz et al.,  
65 2014, 2006, 2000).

66 Up to the isthmus reservoir, the sperm's trip seems to be in a one-way direction.  
67 However, after detaching from the isthmus epithelium, the spermatozoon does not  
68 seem to follow a predetermined route. Finding the precise location of an egg at the  
69 fertilisation site is a major challenge for a cell without a "GPS". Fortunately, the egg  
70 environment expresses widgets that help the spermatozoon to reach the egg. Its  
71 transportation inside the oviduct is influenced by the movement and viscosity of the  
72 oviduct fluid, peristalsis, its confinement in small oviduct spaces, its physiological

73 state, and several aligning and guiding navigation mechanisms. Together, these  
74 factors seem to orchestrate the regulation of fertilisation, not only facilitating  
75 gamete encounter but also preventing the entry of supernumerary spermatozoa to  
76 the egg.

77

## 78 **2. Conditions affecting sperm movement**

79 The spermatozoon is propelled by the flagellum (Lindemann and Lesich, 2016;  
80 Ounjai et al., 2012), which is a complex structure connected to the sperm head by  
81 the neck. It can be divided into three regions: midpiece, principal piece and end  
82 piece. It contains a central axoneme which extends up to the end of the principal  
83 piece. The axoneme has 9 microtubule doublets, connected to a central pair of  
84 microtubules by radial spokes. There are 9 outer dense fibres (ODF), which  
85 externally surround each microtubule doublet. The ODF are encircled by the  
86 mitochondria sheath along the midpiece and by the fibrous sheath along the  
87 principal piece. The propelling force of the flagellum is generated by the hydrolysis  
88 of ATP, mediated by dynein motor proteins that are anchored to each microtubule  
89 doublet, producing a sliding movement between microtubules. However, as the  
90 microtubules are fixed to the neck, a bending movement is generated and a wave  
91 is propagated along the flagellum, the shape of which is determined by the force  
92 provided by the dynein, the ODF, the fibrous sheath structure, and the  
93 hydrodynamic drag force of the fluid in which the spermatozoon is moving  
94 (Lindemann and Lesich, 2016).

95 Sperm trajectories in quasi two-dimensional confinement enabled three different  
96 patterns of movement to be identified, which may reflect different physiological

97 states (Mortimer and Mortimer, 1990): progressive, where the flagellum adopts a  
98 helical movement which propels sperm forward (Mortimer and Mortimer, 1990);  
99 transitional (Fabro et al., 2002; Suarez, 1988), where the flagellum moves with a  
100 wider amplitude but the spermatozoon still swims progressively; and  
101 hyperactivated, characterised by large amplitude bending of the flagellum, which in  
102 turn generates a non-progressive tumbling motion (Mortimer and Mortimer, 1990;  
103 Yanagimachi, 1970). However, the confinement conditions should be taken into  
104 consideration because interaction with walls affects sperm movement. For  
105 instance, sperm swimming up to 1  $\mu\text{m}$  from a solid surface showed a slithering  
106 movement, with a planar flagellar bending with no head rotation, resulting in a  
107 circular sperm trajectory (Guidobaldi et al., 2015; Nosrati et al., 2015). But when  
108 the spermatozoon swims up to 4  $\mu\text{m}$  from the surface, it shows a helical flagellar  
109 beating with a rotating head, and the typical forward progressive trajectory  
110 (Guidobaldi et al., 2015; Nosrati et al., 2015). When spermatozoa are constrained  
111 by top, bottom and lateral walls under ultra-confinement conditions (e.g., at the  
112 edge of microchannel), they swim following the shape of the border delimited by  
113 the lateral walls (Guidobaldi et al., 2014; Lord Rothschild, 1963), with a partial  
114 decrease in progressive velocity (Guidobaldi et al., 2015; Bettera Marcat et al.,  
115 2020). However, spermatozoa swimming far from surfaces without flagellar  
116 movement restriction show a three-dimensional helical or twisted ribbon pattern  
117 (Su et al., 2012, 2013).

118 Another factor directly influencing sperm motility is the viscosity of the medium, as  
119 this can affect the features of flagellum movement (i.e. planarity, torsion,  
120 waveform) without altering the progressive velocity (Kirkman-Brown and Smith,

121 2011; Smith et al., 2009). It is interesting to note that, under *in vivo* conditions,  
122 sperm velocity decreases when it is near to the oviduct wall (Wang and Larina,  
123 2018a). The pattern of sperm movement is thus a consequence of the flagellar  
124 architecture, the medium viscosity, the conditions of confinement and the  
125 interaction with surfaces, which influence the directionality of the spermatozoon.

126

### 127 **3. Oviduct complexity**

128 The oviduct is an intricate three-dimensional organ with several functional and  
129 morphological regions: the uterus-tubal junction, the isthmus, the isthmus-  
130 ampullary junction, the ampulla, and the infundibulum, which are described below  
131 (Fig. 1; Burkitt et al., 2011; Yániz et al., 2014, 2006, 2000). The oviduct presents a  
132 variable number of longitudinal folds, delimiting the oviduct lumen, which is filled  
133 with oviductal fluid (Koyama et al., 2016; Shi et al., 2014). Thus, in the uterus-tubal  
134 junction, the primary folds are flat and wide, and are linked by prominent oblique  
135 secondary folds, which form cul-de-sac-like structures open towards the uterus.  
136 The areas between the folds have shallow pockets with narrow crypts. In the  
137 isthmus, there are four to six primary folds that rarely converge or diverge. An  
138 oblique secondary branching can be observed from the apex to the base of the  
139 primary folds, and becomes more transverse towards the ampullary-isthmic  
140 junction. At the base of the folds, there are flat shallow pockets towards the uterus  
141 that occasionally contain tight crypts. In the ampullary-isthmic junction the principal  
142 folds are interconnected by lateral bifurcated branches that are organised in rows  
143 perpendicular to the principal folds, with irregular grooves between them. In the  
144 ampulla, the longitudinal folds become undulated and increase in number and size

145 towards the infundibulum. Six to ten principal folds can be observed (up to 1300  
146  $\mu\text{m}$  high) alternating with lower folds (up to 500  $\mu\text{m}$  high). The intricate branching in  
147 the ampulla leads to a thin lumen between folds of about tens of micrometres, as  
148 observed in histology slides (Yániz et al., 2014, 2006, 2000), but can be thicker  
149 under *in vivo* conditions (Burton et al., 2015). At the upper end of the ampulla,  
150 there is the Infundibulum, which has a funnel shape. The proximal end of the  
151 infundibulum presents numerous tortuous folds in continuity with those from the  
152 ampulla. Then, they diverge and become less sharp and lower in height towards  
153 the wider opening of the infundibulum. Between the primary folds, there are oblique  
154 secondary folds forming cul-de-sac structures, open in the ovarian direction. Thus,  
155 the lumen spaces along the oviduct become very narrow, generating micro-  
156 confinement spaces for gamete transport and storage. The particularities of its  
157 anatomy and histology make the oviduct a complicated organ for transporting  
158 gametes and embryos.

159

#### 160 **4. Oviduct fluid movement**

161 The epithelium of the oviduct consists of ciliated and secretory cells. The  
162 proportion of these cells varies among regions, with a larger number of secretory  
163 cells in the isthmus, and ciliated cells predominant in the ampulla and infundibulum  
164 (Abe, 1996; Stewart and Behringer, 2012), while the numbers are also influenced  
165 by the cyclic hormonal changes (Abe, 1996). Even though the oviduct physiology  
166 experiences particular changes during the hormonal cycle, to describe the  
167 movement of the oviduct fluid we refer only to the periovulatory period. The fluid  
168 moves inside the oviduct because of the activity of secretory cells, the beating of



169 cilia from ciliated cells, and the oviduct muscle contractility or peristalsis, all of  
170 which are cyclically regulated by sex hormones (Fig. 2; Hunter, 2012). The  
171 oviductal fluid is produced by the contribution of the serum exudate coming from  
172 the blood-oviductal barrier and the exocytic activity of the oviduct secretory cells  
173 (Hunter, 2012). The amount of oviduct fluid during oestrous varies according to the  
174 species secretion rate (Gott et al., 1988; Hino and Yanagimachi, 2019; Iritani et al.,  
175 1974). The movement of the oviduct fluid also depends on cilia beating in the multi-  
176 ciliated cells, which are organised in patches of different sizes, beating  
177 synchronically at a rate below 25 Hz along the longitudinal axis of the oviduct  
178 towards the uterus (Koyama et al., 2019; Shi et al., 2014; Wang et al., 2015; Wang  
179 and Larina, 2018b). The orientation of the ciliary beating current is maintained  
180 towards the uterus in the ampulla in most of the species. However, in the isthmus,  
181 the cilia beating current may be towards the uterus (human, cow, and sheep), pro-  
182 ovarian (pig and rabbit) or not detected (guinea pig and rat) (Gaddum-Rosse et al.,  
183 1973; Gaddum-Rosse and Blandau, 1976; Gaddum-Rosse and Blandau, 1973). In  
184 the isthmus, the cilia movement generates turbulence that moves fluid from the  
185 bottom of the folds, while a current is formed in the middle of the lumen by the cilia  
186 located in the apical ridge of the folds. In contrast, in the ampulla, where the folds  
187 are larger, the main fluid current is observed along the lumen between folds (Kölle  
188 et al., 2009). In addition, the ovulated egg is transported from the infundibulum to  
189 the fertilisation site by cilia beating (Halbert et al., 1989, 1976). Peristalsis consists  
190 of alternate contraction and relaxation of the smooth muscle cells of the oviduct, an  
191 effect that is propagated like a wave along the oviduct. As a consequence, in the  
192 isthmus, the oviductal fluid is pushed in drops back and forwards, with a net

193 advance in the ovary direction, while the movement in the ampulla is unidirectional  
194 towards the peritoneal cavity, at least in the mouse (Battalia and Yanagimachi,  
195 1980, 1979; Blandau and Gaddum Rosse, 1974; see supplementary video 1 in  
196 Guidobaldi et al., 2012; see videos in Hino and Yanagimachi, 2019). Hence, the  
197 net fluid flow depends on the combination of these three factors.

198

## 199 **5. Sperm sweeping by oviduct fluid movement**

200 The complex movement of the oviduct fluid described above apparently influences  
201 sperm transportation to the fertilisation site. However, under natural conditions, the  
202 distribution of spermatozoa along the oviduct is heterogeneous. Most of the  
203 spermatozoa are observed along the isthmus, while few are present at the  
204 fertilisation site (Guidobaldi et al., 2012; Hino and Yanagimachi, 2019; Ishikawa et  
205 al., 2016; La Spina et al., 2016). The back and forward fluid movement spreads  
206 spermatozoa along the isthmus, moving a few of them to the fertilisation site.

207 Indeed, when peristalsis was inhibited, the few spermatozoa found at the  
208 fertilisation site were halved, suggesting that peristalsis contributes to some extent  
209 to transporting sperm to the fertilisation site (Guidobaldi et al., 2012). Other  
210 mechanisms may thus be cooperating to facilitate the gamete encounter.

211

## 212 **6. Sperm taxis towards and away from the egg**

213 Several somatic cells can migrate, for instance, during embryonic development,  
214 wound healing and immune responses, processes in which cell guidance is  
215 modulated by several transportation mechanisms, known as “taxes”,. Spermatozoa  
216 are also sensitive to taxes, i.e, rheotaxis, thermotaxis, and chemotaxis (which may

217 attract or repel the spermatozoon). Rheotaxis refers to sperm alignment according  
218 to the fluid flow, so that when the fluid flows against the sperm head it is called  
219 positive rheotaxis (Fig. 3A). Thermotaxis is sperm movement oriented by gradual  
220 differences in temperature towards the warmest place (Fig. 3B). In chemotaxis, cell  
221 orientation is mediated by the substance concentration gradient, and is positive  
222 when the sperm move towards the source of the substance (chemoattraction,  
223 hereinafter referred to as chemotaxis as it is commonly known), or negative, when  
224 they move away from it (chemorepulsion) (Fig. 3C). We next describe what is  
225 known about these sperm transportation mechanisms.

### 226 **6.a. Sperm rheotaxis**

227 Sperm rheotaxis was first reported by Bretherton and Rothschild (1961), and to  
228 date has been characterised in humans (Bretherton and Lord Rothschild, 1961; De  
229 Martin et al., 2017; Miki and Clapham, 2013; Zhang et al., 2016), bulls (Bretherton  
230 and Lord Rothschild, 1961; El-Sherry et al., 2017, 2014; Johnson et al., 2017),  
231 mice (Miki and Clapham, 2013), stallions and boars (Fair and Romero-  
232 Aguirregomezcorta, 2019; Romero-Aguirregomezcorta et al., 2018). It seems that  
233 rheotaxis selects motile spermatozoa regardless of the physiological state, since  
234 both non-capacitated and capacitated spermatozoa immersed in low- and high-  
235 viscosity media elicit rheotactic behaviour, aligning their movement against the fluid  
236 flow current (Miki and Clapham, 2013). The rheotactic sperm pattern is  
237 characterised by an increase in velocity (Rappa et al., 2018), rotation of the tail and  
238 hyperactivated behaviour (Miki and Clapham, 2013). A three-dimensional study  
239 also shows that the cell's turning direction is defined by the asymmetrical  
240 movement of the flagellum midpiece (Bukatin et al., 2015). Interestingly, studies

241 based on sperm movement simulation under flow predicted that rheotaxis is  
242 dependent on sperm confinement (Ishimoto and Gaffney, 2015) and surface  
243 interactions (Kantsler et al., 2014). The changes in motility associated with  
244 rheotaxis seem to be accompanied by extracellular calcium mobilisation by means  
245 of the CatSper channel (Miki and Clapham, 2013). In addition, bull spermatozoa  
246 best express rheotaxis at pH 6.4–6.6, the range at which constant values of nitric  
247 oxide, potassium and calcium are observed (El-Sherry et al., 2017). However,  
248 other authors report that there are no significant differences in sperm flagellar  
249 beating amplitude and asymmetry and that no calcium influx was observed during  
250 sperm rheotaxis turning (Zhang et al., 2016).

#### 251 **6.b. Sperm thermotaxis**

252 This behaviour was first described almost 20 years ago in a small subpopulation of  
253 capacitated rabbit spermatozoa; consistently, the ampulla is about 2°C warmer  
254 than the isthmus region of the oviduct (Bahat et al., 2003). This temperature  
255 difference is enhanced in the periovulatory phase in the rabbit (Bahat et al., 2005).  
256 Intriguingly, human spermatozoa can respond to temperature gradients as low as  
257 0.014°C/mm (Bahat et al., 2012). The sperm pattern of thermotactic movement  
258 involves changes in the frequency of turns and sperm velocity while searching for  
259 the temperature gradient; but when it is found, the values of those sperm  
260 parameters decrease, and the spermatozoon begins swimming straightforwardly  
261 aligned with the temperature gradient (Boryshpolets et al., 2015). The thermotaxis  
262 signalling mechanism seems to be initiated by the activation of the opsins (G-  
263 protein-coupled receptors), rhodopsin and melanopsin, which are co-localised  
264 mainly in the sperm head membrane in human and mouse spermatozoa (Pérez-

265 Cerezales et al., 2015; Roy et al., 2020). The rhodopsin receptor is involved in the  
266 cyclic-nucleotide pathway and the melanopsin activates the phospholipase C  
267 pathway (Bahat and Eisenbach, 2010; Pérez-Cerezales et al., 2015; Roy et al.,  
268 2020). Moreover, the transient receptor potential vanilloid (TRPV1 and TRPV4) has  
269 also been reported to mediate sperm thermotaxis in mice (Hamano et al., 2016)  
270 and humans (De Toni et al., 2016). The phospholipase C pathway may also  
271 reinforce the activity of TRPV1 (De Toni et al., 2016).

### 272 **6.c. Sperm chemoattraction**

273 In mammals, sperm chemotaxis was first reported for human spermatozoa towards  
274 peptides that attract bacteria (Gnessi et al., 1985). A few years later it was reported  
275 that human spermatozoa were attracted by follicular fluid from fertile oocytes (Ralt  
276 et al., 1991). This positioned sperm chemotaxis as an interesting mechanism that  
277 had the potential to improve the outcome of ART. It has so far been observed in  
278 small subpopulations of capacitated human, mouse, rabbit, bovine and equine  
279 spermatozoa (Dominguez, 2019; Dominguez et al., 2018; Eisenbach and Giojalas,  
280 2006; Giojalas et al., 2015; Moreno-Irusta et al., 2020). The chemotactic response  
281 lasts up to two hours (Cohen-Dayag et al., 1995; Fabro et al., 2002), fluctuating  
282 with an ultradian cycle of two hours, and also with an infradian seasonal rhythm, at  
283 least in humans (Moreno-Irusta et al., 2019). Interestingly, the chemotactic state is  
284 associated with the time a fertilisable oocyte is available in the oviduct. Thus, in  
285 humans where ovulation does not necessarily coincide with ejaculation, the  
286 capacitated-chemotactic state is prolonged over time, but in the rabbit, where  
287 ovulation occurs upon the stimulus of coitus, it lasts a few hours (Giojalas et al.,  
288 2004). In addition, the acrosome must be intact for the occurrence of sperm

289 chemotaxis (Fabro et al., 2002; Guidobaldi et al., 2017b). Concerning the  
290 chemotactic pattern, capacitated spermatozoa swimming in a spatial concentration  
291 gradient orient their movement towards the source of the attractant with a  
292 transitional forward pattern (Blengini et al., 2011). But when the spermatozoon is  
293 aligned to the gradient, it swims straight forward, with turns and hyperactivation  
294 being suppressed (Armon and Eisenbach, 2011; Ernesto et al., 2015).

295 The first biological source of chemoattractants was follicular fluid in humans (Ralt  
296 et al., 1991) and mice (Oliveira et al., 1999). Other sources, like oviductal fluid in  
297 mice (Oliveira et al., 1999), the cumulus oophorus in humans (Oren-Benaroya et  
298 al., 2008; Sun et al., 2005) and rabbits (Guidobaldi et al., 2008), and the egg in  
299 humans (Sun et al., 2005), were also reported. But these sources are usually a  
300 mixture of molecules of different chemical nature, like hormones, peptides, reactive  
301 species, etc, some of which have been tested for chemotaxis.

302 Atrial natriuretic peptide is present in oviductal and follicular fluids and was  
303 reported to chemoattract human and mouse spermatozoa (Anderson et al., 1995;  
304 Bian et al., 2012; Zamir et al., 1993). Several chemokines and cysteine-rich  
305 secretory proteins, produced by granulosa, cumulus cells and/or the egg, have  
306 been reported to chemoattract human or mouse spermatozoa (Ernesto et al., 2015;  
307 Giojalas et al., 2015) and the corresponding receptor for some of these was  
308 identified in spermatozoa (Giojalas et al., 2015). Progesterone is a steroid secreted  
309 by the cumulus cells from the time of ovulation (Bar-Ami et al., 1989; Vanderhyden  
310 and Tonary, 1995) and was reported to induce chemotaxis upon gradients of low  
311 concentration (picomolar range) in human (Blengini et al., 2011; Gatica et al.,  
312 2013; Guidobaldi et al., 2017a; Teves et al., 2010, 2009, 2006), rabbit (Guidobaldi

313 et al., 2017a; Teves et al., 2006), mouse (Ernesto et al., 2015; Guidobaldi et al.,  
314 2017a, 2017b), bovine (Dominguez et al., 2018) and equine (Dominguez, 2019)  
315 spermatozoa, the chemotactic activity of which is modulated by the corticosteroid-  
316 binding globulin (Teves et al., 2010). The chemotactic response of sperm to  
317 progesterone seems to be mediated by a surface receptor located in the head  
318 (rabbit) or tail (human) (Guidobaldi et al., 2008). Even though several membrane  
319 proteins have been claimed as progesterone receptors (Giojalas et al., 2015; Miller  
320 et al., 2016), none of these studies provided experimental evidence of the  
321 participation of those proposed progesterone receptors in the chemotactic  
322 response of sperm. Nitric oxide, a free radical with a brief lifespan, secreted by the  
323 cumulus cells (Bu et al., 2003), chemoattracts human spermatozoa (Miraglia et al.,  
324 2007); interestingly, spermatozoa also release this molecule (Lewis et al., 1996),  
325 and thus a homologous attraction cannot be discarded. Odorant substances have  
326 been also reported to attract human and mouse spermatozoa (Fukuda et al., 2004;  
327 Spehr et al., 2003; Veitinger et al., 2011), and the presence of odorant receptors  
328 was described in spermatozoa (Fukuda et al., 2004; Spehr et al., 2003). However,  
329 the natural source of odorants in the female genital tract is not known. Cyclic  
330 nucleotides and reactive oxygen species are second messengers in chemotaxis  
331 signalling (Miraglia et al., 2007; Moreno-Irusta et al., 2020; Teves et al., 2009).  
332 Moreover, when spermatozoa are exposed to a concentration gradient of these  
333 small molecules, they emulate the action of a chemoattractant as reported for  
334 human (Teves et al., 2009) and equine (Moreno-Irusta et al., 2020) spermatozoa.  
335 Therefore, the use of concentration gradients of these molecules is an interesting  
336 tool to investigate the chemotactic molecular mechanism; however, they cannot be

337 considered putative attractants. There are also attractants of unknown chemical  
338 identity that have been isolated from follicular fluid or the oocyte, which can  
339 stimulate human sperm chemotaxis (Armon et al., 2014; Ralt et al., 1994).  
340 Studies of chemotactic signalling have examined the attractants, progesterone,  
341 nitric oxide, odorants, and atrial natriuretic peptide. Interestingly, the pathways  
342 studied in each case are elicited by more than one attractant. In general, signalling  
343 has been reported via adenylyl cyclase - cyclic adenosine monophosphate -  
344 protein kinase A and via guanylate cyclase - cyclic guanosine monophosphate -  
345 protein kinase C, reactive oxygen species, protein phosphorylation in tyrosine and  
346 calcium mobilisation from different origins (see Fig.3 in Giojalas et al., 2015;  
347 Moreno-Irusta et al., 2020)

#### 348 **6.d. Sperm chemorepulsion**

349 Sperm repulsion has been observed in human, rabbit and mouse spermatozoa,  
350 sharing several characteristics with sperm chemotaxis. For instance, only the small  
351 subpopulation of capacitated spermatozoa can respond with repulsion, which is  
352 characterised by orientation of its movement away from the source of a substance,  
353 swimming with a transitional pattern (Guidobaldi et al., 2017a). The repellents  
354 tested so far are synthetic, like progesterone receptor ligands (sPRL) that are used  
355 as contraceptives (mifepristone, levonorgestrel, and ulipristal acetate), or  
356 physiological, like zinc released immediately and transiently after fertilisation (Kim  
357 et al., 2011; Que et al., 2017), suggesting an effect for blocking polyspermy.  
358 Indeed, rabbit spermatozoa treated with ulipristal are prevented from reaching the  
359 oocyte surface (Guidobaldi et al., 2017a). Interestingly, chemorepulsion was also  
360 observed when spermatozoa were exposed simultaneously to a concentration



361 gradient of progesterone (at the picomolar chemotactic range) and to a  
362 homogeneous distribution of sPRL or zinc. Thus, the chemotactic gradient of  
363 progesterone is converted by sPRL or zinc into a repellent gradient (Guidobaldi et  
364 al., 2017a). The molecular signalling of sperm chemorepulsion seems to be like  
365 that described for chemotaxis towards progesterone (unpublished data from our  
366 lab).

367

## 368 **7. A theoretical model to explain sperm transportation to and away from** 369 **the egg**

370 The complexity of spatial-temporal oviduct architecture and functionality led to the  
371 notion that the sperm's own motility is not sufficiently capable of reaching the  
372 oocyte surface, and that extra guiding mechanisms may help to accomplish this  
373 goal. Based on the literature mentioned in this review, we propose a general  
374 theoretical model to explain how spermatozoa manage to complete this journey,  
375 particularly from the isthmus sperm reservoir to the oocyte membrane (Fig. 4),  
376 though there may be variations between species. The few spermatozoa that  
377 accomplish capacitation are released from the epithelium of the oviduct reservoir.  
378 Then, the cilia beating moves the spermatozoa from the bottom towards the ridge  
379 of the folds, where they are exposed to the current of oviduct fluid and peristalsis,  
380 which transport spermatozoa in the ad-ovarian direction. During oviduct  
381 contraction, spermatozoa may be transported inside drops of oviduct fluid along  
382 the isthmus; however, during oviduct relaxation, the oviductal fluid current is  
383 maintained by cilia beating towards the uterus, thus orienting the sperm by  
384 rheotaxis. It is interesting to note that the number of spermatozoa that are

385 transported along the isthmus is drastically decreased to tens in the ampulla. This  
386 may be due, in part, to the increase in the number of folds and the lumen surface,  
387 which may create resistance to the movement of the fluid by peristalsis coming  
388 from the isthmus. The complexity of the ampulla provides numerous alternative  
389 pathways between the folds, where interaction with the oviduct surface in micro-  
390 confined spaces guides the spermatozoon to swim next to the walls along the  
391 folds. Upon ovulation, the egg enters the infundibulum and is carried towards the  
392 fertilisation site by cilia beating, where it remains in one of the multiple intricate  
393 spaces between folds. In such a labyrinthine scenario, how can gametes encounter  
394 each other? Peristalsis, thermotaxis, and rheotaxis may move spermatozoa along  
395 the ampullary lumen. But since none of these mechanisms can guide the  
396 spermatozoon to the precise location of the egg, the gamete encounter would be  
397 by chance. Thus, spermatozoa may find the particular pathway where the egg is  
398 located by chemotaxis. During relaxation, concentration gradients of  
399 chemoattractants secreted by the egg may be spread by cilia beating along the  
400 small lumen between folds, increasing the probabilities of gamete encounter. But  
401 the spermatozoa must still penetrate the egg vestments to reach the oocyte  
402 surface. This step may be operated by chemotaxis due to the gradual secretion of  
403 one or more chemoattractants, either from the cumulus cells or the oocyte. Once  
404 fertilised, the oocyte secretes zinc which, in combination with the progesterone  
405 gradient, would rapidly repel arriving capacitated spermatozoa, preventing the  
406 entry of additional sperm cells. This complex interplay suggests to us that the  
407 intricate oviduct structure evolved in association with a multiplicity of sperm-guiding

408 mechanisms not only to ensure the gamete encounter but also to guarantee that  
409 one oocyte is fertilised by only one spermatozoon.

410

411 **8. Can sperm taxis be applied as a technological tool to improve or to**  
412 **prevent fertilisation?**

413 Even though the participation *in vivo* of these taxes has not yet been fully  
414 demonstrated, their ability to select spermatozoa in a better physiological state has  
415 encouraged the development of methods that may improve ART outcomes in  
416 humans and animals. For instance, microfluidic devices based on fluid flow select  
417 spermatozoa by rheotaxis, providing them with higher fertilisation ability,  
418 morphology, motility or low uncondensed chromatin (De Martin et al., 2017; Hwang  
419 et al., 2019; Zaferani et al., 2018). In any event, further studies are needed to test  
420 whether the spermatozoa selected by rheotaxis indeed improve the ART outcome.  
421 In thermotaxis, sperm quality is favoured by temperature selection since faster  
422 spermatozoa have been obtained with less damaged DNA (Pérez-Cerezales et al.,  
423 2018). Moreover, spermatozoa isolated by thermotaxis were used to fertilise mice  
424 oocytes, giving rise to a greater number of good quality embryos and pregnancies  
425 (Pérez-Cerezales et al., 2018). In the case of chemotaxis, spermatozoa selected  
426 by the chemoattractant progesterone elicited a higher level of capacitation, and  
427 lower DNA fragmentation and oxidative stress (Dominguez, 2019; Dominguez et  
428 al., 2018; Gatica et al., 2013). Moreover, when spermatozoa selected by  
429 chemotaxis towards progesterone were used to fertilise the oocyte by different  
430 ART procedures, an improvement was observed in the rate of cleavage or embryo  
431 quality (Dominguez, 2019; Dominguez et al., 2018). Thus, to improve the outcome

432 of ART, simple devices and procedures may be designed to select the best  
433 spermatozoa by means of one or more sperm taxes (perhaps combined with some  
434 oviductal features), without much perturbing the ART logistics. Some attempts  
435 have already been made in this direction (Bhagwat et al., 2018; Ko et al., 2018).  
436 And for contraception purposes, new protocols based on sperm repulsion may be  
437 designed to prevent gamete encounter without secondary effects.

438

## 439 **9. Conclusions and future perspectives**

440 Knowledge of the factors influencing sperm arrival at the egg has increased in  
441 recent decades, suggesting a much more complex scenario than that imagined in  
442 the past. Considering that sperm capacitation and sperm transport mediated by  
443 taxis are closely related, being able to obtain a subpopulation containing  
444 capacitated sperm provides a model to better comprehend the dynamics between  
445 the capacitated and post-capacitated state. The molecular level fine-tuning that  
446 regulates the orchestration of sperm transport towards and away from the egg still  
447 needs much further research. Another intriguing issue is the possibility that the  
448 female chooses the best spermatozoon, a hypothesis postulated that must be  
449 tested at molecular level. As a whole, such knowledge would not only illuminate  
450 the mechanisms underlying the regulation of fertilisation but also enable the  
451 manipulation of sperm transport for biotechnological purposes.

452

## 453 **10. Acknowledgements**

454 LCG and HAG are researchers from the Consejo Nacional de Investigaciones  
455 Científicas y Técnicas (Argentina). Research received financial support from

456 Universidad Nacional de Córdoba (2018-2022) and Agencia Nacional de  
457 Promoción Científica (PID C 0016-2014).

458

## 459 11. References

- 460 Abe, H., 1996. The mammalian oviductal epithelium: regional variations in cytological and  
461 functional aspects of the oviductal secretory cells. *Histol. Histopathol.* 11, 743–68.
- 462 Anderson, R. a, Feathergill, K. a, Rawlins, R.G., Mack, S.R., Zaneveld, L.J., 1995. Atrial  
463 natriuretic peptide: a chemoattractant of human spermatozoa by a guanylate cyclase-  
464 dependent pathway. *Mol. Reprod. Dev.* 40, 371–8.  
465 <https://doi.org/10.1002/mrd.1080400314>
- 466 Armon, L., Ben-Ami, I., Ron-El, R., Eisenbach, M., 2014. Human oocyte-derived sperm  
467 chemoattractant is a hydrophobic molecule associated with a carrier protein. *Fertil.*  
468 *Steril.* <https://doi.org/10.1016/j.fertnstert.2014.06.011>
- 469 Armon, L., Eisenbach, M., 2011. Behavioural mechanism during human sperm chemotaxis:  
470 involvement of hyperactivation. *PLoS One* 6, e28359.  
471 <https://doi.org/10.1371/journal.pone.0028359>
- 472 Bahat, A., Caplan, S.R., Eisenbach, M., 2012. Thermotaxis of human sperm cells in  
473 extraordinarily shallow temperature gradients over a wide range. *PLoS One* 7, 1–9.  
474 <https://doi.org/10.1371/journal.pone.0041915>
- 475 Bahat, A., Eisenbach, M., 2010. Human sperm thermotaxis is mediated by phospholipase C  
476 and inositol trisphosphate receptor Ca<sup>2+</sup> channel. *Biol. Reprod.* 82, 606–16.  
477 <https://doi.org/10.1095/biolreprod.109.080127>
- 478 Bahat, A., Eisenbach, M., Tur-Kaspa, I., 2005. Periovulatory increase in temperature  
479 difference within the rabbit oviduct. *Hum. Reprod.* 20, 2118–2121.  
480 <https://doi.org/10.1093/humrep/dei006>
- 481 Bahat, A., Tur-Kaspa, I., Gakamsky, A., Giojalas, L.C., Breitbart, H., Eisenbach, M., 2003.  
482 Thermotaxis of mammalian sperm cells: a potential navigation mechanism in the  
483 female genital tract. *Nat. Med.* 9, 149–50. <https://doi.org/10.1038/nm0203-149>
- 484 Bar-Ami, S., Gitay-Goren, H., Brandes, J.M., 1989. Different morphological and  
485 steroidogenic patterns in oocyte/cumulus-corona cell complexes aspirated at in vitro  
486 fertilization. *Biol. Reprod.* 41, 761–70.
- 487 Battalia, D.E., Yanagimachi, R., 1980. The change in oestrogen and progesterone levels  
488 triggers adovarian propulsive movement of the hamster oviduct. *J. Reprod. Fertil.* 59,  
489 243–7.
- 490 Battalia, D.E., Yanagimachi, R., 1979. Enhanced and co-ordinated movement of the  
491 hamster oviduct during the periovulatory period. *J. Reprod. Fertil.* 56, 515–20.  
492 <https://doi.org/10.1530/jrf.0.0560515>
- 493 Bettera Marcat, M.A., Gallea, M.N., Miño, G.L., Cubilla, M.A., Banchio, A.J., Giojalas,

- 494 L.C., Marconi, V.I., Guidobaldi, H.A., 2020. Hitting the wall: Human sperm velocity  
495 recovery under ultra-confined conditions. *Biomicrofluidics* 14, 024108.  
496 <https://doi.org/10.1063/1.5143194>
- 497 Bian, F., Mao, Guankun, Guo, M., Mao, Guanping, Wang, J., Li, J., Han, Y., Chen, X.,  
498 Zhang, M., Xia, G., 2012. Gradients of natriuretic peptide precursor A (NPPA) in  
499 oviduct and of natriuretic peptide receptor 1 (NPR1) in spermatozoon are involved in  
500 mouse sperm chemotaxis and fertilization. *J. Cell. Physiol.* 227, 2230–2239.  
501 <https://doi.org/10.1002/jcp.22962>
- 502 Blandau, R.J., Gaddum Rosse, P., 1974. Mechanism of sperm transport in pig oviducts.  
503 *Fertil. Steril.* 25, 61–67. [https://doi.org/10.1016/S0015-0282\(16\)40154-8](https://doi.org/10.1016/S0015-0282(16)40154-8)
- 504 Blengini, C.S., Teves, M.E., Uñates, D.R., Guidobaldi, H.A., Gatica, L.V., Giojalas, L.C.,  
505 2011. Human sperm pattern of movement during chemotactic re-orientation towards a  
506 progesterone source. *Asian J. Androl.* 13, 769–73. <https://doi.org/10.1038/aja.2011.27>
- 507 Boryshpolets, S., Pérez-Cerezales, S., Eisenbach, M., 2015. Behavioral mechanism of  
508 human sperm in thermotaxis: A role for hyperactivation. *Hum. Reprod.* 30, 884–892.  
509 <https://doi.org/10.1093/humrep/dev002>
- 510 Boyd, K.L., Muehlenbachs, A., Rendi, M.H., Garcia, R.L., Gibson-Corley, K.N., 2018.  
511 Female Reproductive System, in: Treuting, P.M., Dintzis, S.M., Montine, K.S.B.T.-  
512 C.A. and H. (Second E. (Eds.), *Comparative Anatomy and Histology*. Elsevier, San  
513 Diego, pp. 303–334. <https://doi.org/10.1016/B978-0-12-802900-8.00017-8>
- 514 Bretherton, F.P., Lord Rothschild, F.R.S., 1961. Rheotaxis of spermatozoa. *Proc. R. Soc.*  
515 *London. Ser. B. Biol. Sci.* 153, 490–502. <https://doi.org/10.1098/rspb.1961.0014>
- 516 Bu, S., Xia, G., Xie, H., Guo, Y., 2003. Nitric oxide produced by cumulus cells stimulates  
517 maturation of mouse oocytes. *Chinese Sci. Bull.* 48, 72–75.  
518 <https://doi.org/10.1360/03tb9015>
- 519 Bukatin, A., Kukhtevich, I., Stoop, N., Dunkel, J., Kantsler, V., 2015. Bimodal rheotactic  
520 behavior reflects flagellar beat asymmetry in human sperm cells. *Proc. Natl. Acad.*  
521 *Sci. U. S. A.* 112, 15904–15909. <https://doi.org/10.1073/pnas.1515159112>
- 522 Burkitt, M., Walker, D., Romano, D.M., Fazeli, A., 2011. Computational modelling of  
523 maternal interactions with spermatozoa: Potentials and prospects. *Reprod. Fertil. Dev.*  
524 23, 976–989. <https://doi.org/10.1071/RD11032>
- 525 Burton, J.C., Wang, S., Stewart, C.A., Behringer, R.R., Larina, I. V., 2015. High-resolution  
526 three-dimensional in vivo imaging of mouse oviduct using optical coherence  
527 tomography. *Biomed. Opt. Express* 6, 2713. <https://doi.org/10.1364/boe.6.002713>
- 528 Cohen-Dayag, A., Tur-Kaspa, I., Dor, J., Mashiach, S., Eisenbach, M., 1995. Sperm  
529 capacitation in humans is transient and correlates with chemotactic responsiveness to  
530 follicular factors. *Proc. Natl. Acad. Sci. U. S. A.* 92, 11039–43.
- 531 De Martin, H., Cocuzza, M.S., Tiseo, B.C., Wood, G.J.A., Miranda, E.P., Monteleone,  
532 P.A.A., Soares, J.M., Serafini, P.C., Srougi, M., Baracat, E.C., 2017. Positive  
533 rheotaxis extended drop: a one-step procedure to select and recover sperm with mature  
534 chromatin for intracytoplasmic sperm injection. *J. Assist. Reprod. Genet.* 34, 1699–  
535 1708. <https://doi.org/10.1007/s10815-017-1024-1>

- 536 De Toni, L., Garolla, A., Menegazzo, M., Magagna, S., Di Nisio, A., Šabović, I., Rocca,  
537 M.S., Scattolini, V., Filippi, A., Foresta, C., 2016. Heat Sensing Receptor TRPV1 Is a  
538 Mediator of Thermotaxis in Human Spermatozoa. *PLoS One* 11, e0167622.  
539 <https://doi.org/10.1371/journal.pone.0167622>
- 540 Dominguez, E.M., 2019. Aplicación del ensayo de selección espermática (ESE) para  
541 optimizar la producción in vitro de embriones equinos y bovinos sexados.  
542 Universidad Nacional de Río Cuarto, Argentina.
- 543 Dominguez, E.M., Moreno-Irusta, A., Guidobaldi, H.A., Tribulo, H., Giojalas, L.C., 2018.  
544 Improved bovine in vitro embryo production with sexed and unsexed sperm selected  
545 by chemotaxis. *Theriogenology* 122, 1–8.  
546 <https://doi.org/10.1016/j.theriogenology.2018.08.023>
- 547 Eddy, E., 2006. The Spermatozoon, in: Neill, J.D.B.T.-K. and N.P. of R. (Third E. (Ed.),  
548 Knobil and Neill's Physiology of Reproduction. Elsevier, St Louis, pp. 3–54.  
549 <https://doi.org/10.1016/B978-012515400-0/50006-3>
- 550 Eisenbach, M., Giojalas, L.C., 2006. Sperm guidance in mammals - an unpaved road to the  
551 egg. *Nat. Rev. Mol. Cell Biol.* 7, 276–85. <https://doi.org/10.1038/nrm1893>
- 552 El-Sherry, T.M., Abdel-Ghani, M.A., Abou-Khalil, N.S., Elsayed, M., Abdelgawad, M.,  
553 2017. Effect of pH on rheotaxis of bull sperm using microfluidics. *Reprod. Domest.*  
554 *Anim.* 52, 781–790. <https://doi.org/10.1111/rda.12979>
- 555 El-Sherry, T.M., Elsayed, M., Abdelhafez, H.K., Abdelgawad, M., 2014. Characterization  
556 of rheotaxis of bull sperm using microfluidics. *Integr. Biol. (United Kingdom)* 6,  
557 1111–1121. <https://doi.org/10.1039/c4ib00196f>
- 558 Ernesto, J.I., Weigel Munoz, M., Battistone, M.A., Vasen, G., Martinez-Lopez, P., Orta, G.,  
559 Figueiras-Fierro, D., De la Vega-Beltran, J.L., Moreno, I.A., Guidobaldi, H.A.,  
560 Giojalas, L., Darszon, A., Cohen, D.J., Cuasnicu, P.S., 2015. CRISP1 as a novel  
561 CatSper regulator that modulates sperm motility and orientation during fertilization. *J.*  
562 *Cell Biol.* 210, 1213–1224. <https://doi.org/10.1083/jcb.201412041>
- 563 Fabro, G., Rovasio, R.A., Civalero, S., Frenkel, A., Caplan, S.R., Eisenbach, M., Giojalas,  
564 L.C., 2002. Chemotaxis of capacitated rabbit spermatozoa to follicular fluid revealed  
565 by a novel directionality-based assay. *Biol. Reprod.* 67, 1565–71.  
566 <https://doi.org/10.1095/biolreprod.102.006395>
- 567 Fair, S., Romero-Aguirregomezcorta, J., 2019. Implications of boar sperm kinematics and  
568 rheotaxis for fertility after preservation. *Theriogenology* 137, 15–22.  
569 <https://doi.org/10.1016/j.theriogenology.2019.05.032>
- 570 Fukuda, N., Yomogida, K., Okabe, M., Touhara, K., 2004. Functional characterization of a  
571 mouse testicular olfactory receptor and its role in chemosensing and in regulation of  
572 sperm motility. *J. Cell Sci.* 117, 5835–45. <https://doi.org/10.1242/jcs.01507>
- 573 Gaddum-Rosse, P., Blandau, R.J., 1976. Comparative observations on ciliary currents in  
574 mammalian oviducts. *Biol. Reprod.* 14, 605–9.
- 575 Gaddum-Rosse, P., Blandau, R.J., Thiersch, J.B., 1973. Ciliary activity in the human and  
576 *Macaca nemestrina* oviduct. *Am. J. Anat.* 138, 269–75.  
577 <https://doi.org/10.1002/aja.1001380210>

- 578 Gaddum-Rosse, P., Blandau, R.J., 1973. In vitro studies on ciliary activity within the  
579 oviducts of the rabbit and pig. *Am. J. Anat.* 136, 91–104.  
580 <https://doi.org/10.1002/aja.1001360108>
- 581 Gatica, L. V., Guidobaldi, H.A., Montesinos, M.M., Teves, M.E., Moreno, a. I., Uñates,  
582 D.R., Molina, R.I., Giojalas, L.C., 2013. Picomolar gradients of progesterone select  
583 functional human sperm even in subfertile samples. *Mol. Hum. Reprod.* 19, 559–69.  
584 <https://doi.org/10.1093/molehr/gat037>
- 585 Giojalas, L.C., Guidobaldi, H.A., Sánchez, R., 2015. Sperm Chemotaxis in Mammals, in:  
586 Cosson, J. (Ed.), *Flagellar Mechanics and Sperm Guidance*. Bentham Science  
587 Publishers, Sharjah, Emiratos Árabes Unidos, pp. 272–307.  
588 <https://doi.org/10.2174/9781681081281115010012>
- 589 Giojalas, L.C., Rovasio, R.A., Fabro, G., Gakamsky, A., Eisenbach, M., 2004. Timing of  
590 sperm capacitation appears to be programmed according to egg availability in the  
591 female genital tract. *Fertil. Steril.* 82, 247–9.  
592 <https://doi.org/10.1016/j.fertnstert.2003.11.046>
- 593 Gnessi, L., Ruff, M.R., Fraioli, F., Pert, C.B., 1985. Demonstration of receptor-mediated  
594 chemotaxis by human spermatozoa. A novel quantitative bioassay. *Exp. Cell Res.* 161,  
595 219–30.
- 596 Gott, A. L., Gray, S.M., James, A. F., Leese, H.J., 1988. The mechanism and control of  
597 rabbit oviduct fluid formation. *Biol. Reprod.* 39, 758–63.
- 598 Guidobaldi, A., Jeyaram, Y., Berdakin, I., Moshchalkov, V. V, Condat, C.A., Marconi,  
599 V.I., Giojalas, L., Silhanek, A. V, 2014. Geometrical guidance and trapping transition  
600 of human sperm cells. *Phys. Rev. E. Stat. Nonlin. Soft Matter Phys.* 89, 032720.  
601 <https://doi.org/10.1103/PhysRevE.89.032720>
- 602 Guidobaldi, H., Cubilla, M., Moreno, A., Molino, M., Bahamondes, L., Giojalas, L., 2017a.  
603 Sperm chemorepulsion, a supplementary mechanism to regulate fertilization. *Hum.*  
604 *Reprod.* 32, 1560–1573. <https://doi.org/10.1093/humrep/dex232>
- 605 Guidobaldi, H., Hirohashi, N., Cubilla, M., Buffone, M., Giojalas, L., 2017b. An intact  
606 acrosome is required for the chemotactic response to progesterone in mouse  
607 spermatozoa. *Mol. Reprod. Dev.* 84, 310–315. <https://doi.org/10.1002/mrd.22782>
- 608 Guidobaldi, H.A., Jeyaram, Y., Condat, C.A., Oviedo, M., Berdakin, I., Moshchalkov, V.  
609 V., Giojalas, L.C., Silhanek, A. V., Marconi, V.I., 2015. Disrupting the wall  
610 accumulation of human sperm cells by artificial corrugation. *Biomicrofluidics* 9,  
611 024122. <https://doi.org/10.1063/1.4918979>
- 612 Guidobaldi, A., Jeyaram, Y., Berdakin, I., Moshchalkov, V. V, Condat, C.A., Marconi,  
613 V.I., Giojalas, L., Silhanek, A. V, 2014. Geometrical guidance and trapping transition  
614 of human sperm cells. *Phys. Rev. E. Stat. Nonlin. Soft Matter Phys.* 89, 032720.  
615 <https://doi.org/10.1103/PhysRevE.89.032720>
- 616 Guidobaldi, H.A., Teves, M.E., Uñates, D.R., Anastasía, A., Giojalas, L.C., 2008.  
617 Progesterone from the cumulus cells is the sperm chemoattractant secreted by the  
618 rabbit oocyte cumulus complex. *PLoS One* 3, e3040.



- 619 <https://doi.org/10.1371/journal.pone.0003040>
- 620 Guidobaldi, H.A., Teves, M.E., Uñates, D.R., Giojalas, L.C., 2012. Sperm transport and  
621 retention at the fertilization site is orchestrated by a chemical guidance and oviduct  
622 movement. *Reproduction* 143, 587–96. <https://doi.org/10.1530/REP-11-0478>
- 623 Halbert, S.A., Becker, D.R., Szal, S.E., 1989. Ovum transport in the rat oviductal ampulla  
624 in the absence of muscle contractility. *Biol. Reprod.* 40, 1131–6.
- 625 Halbert, S.A., Tam, P.Y., Blandau, R.J., 1976. Egg transport in the rabbit oviduct: the roles  
626 of cilia and muscle. *Science* 191, 1052–3.
- 627 Hamano, K.I., Kawanishi, T., Mizuno, A., Suzuki, M., Takagi, Y., 2016. Involvement of  
628 transient receptor potential vanilloid (TRPV) 4 in mouse sperm thermotaxis. *J.*  
629 *Reprod. Dev.* 62, 415–422. <https://doi.org/10.1262/jrd.2015-106>
- 630 Harper, M. J. K., C. R. Austin y R. V. Short., 1982. Sperm and egg transport. *Reproduction*  
631 in mammals. Germ cells and fertilization. Cambridge, Cambridge University Press.  
632 2nd Edition, 102-127.
- 633 Hino, T., Yanagimachi, R., 2019. Active peristaltic movements and fluid production of the  
634 mouse oviduct: their roles in fluid and sperm transport and fertilization. *Biol. Reprod.*  
635 101, 40–49. <https://doi.org/10.1093/biolre/iox061>
- 636 Hunter, R.H.F., 2012. Components of oviduct physiology in eutherian mammals. *Biol. Rev.*  
637 87, 244–255. <https://doi.org/10.1111/j.1469-185X.2011.00196.x>
- 638 Hwang, J.Y., Mannowetz, N., Zhang, Y., Everley, R.A., Gygi, S.P., Bewersdorf, J., Lishko,  
639 P. V., Chung, J.-J., 2019. Dual Sensing of Physiologic pH and Calcium by EFCAB9  
640 Regulates Sperm Motility. *Cell* 1–15. <https://doi.org/10.1016/j.cell.2019.03.047>
- 641 Iritani, A., Sato, E., Nishikawa, Y., 1974. Secretion rates and chemical composition of  
642 oviduct and uterine fluids in sows. *J. Anim. Sci.* 39, 582–8.  
643 <https://doi.org/10.2527/jas1974.393582x>
- 644 Ishikawa, Y., Usui, T., Yamashita, M., Kanemori, Y., Baba, T., 2016. Surfing and  
645 Swimming of Ejaculated Sperm in the Mouse Oviduct. *Biol. Reprod.* 94, 1–9.  
646 <https://doi.org/10.1095/biolreprod.115.135418>
- 647 Ishimoto, K., Gaffney, E.A., 2015. Fluid flow and sperm guidance: A simulation study of  
648 hydrodynamic sperm rheotaxis. *J. R. Soc. Interface* 12.  
649 <https://doi.org/10.1098/rsif.2015.0172>
- 650 Johnson, G.P., English, A.M., Cronin, S., Hoey, D.A., Meade, K.G., Fair, S., 2017.  
651 Genomic identification, expression profiling, and functional characterization of  
652 CatSper channels in the bovine. *Biol. Reprod.* 97, 302–312.  
653 <https://doi.org/10.1093/biolre/iox082>
- 654 Kantsler, V., Dunkel, J., Blayney, M., Goldstein, R.E., 2014. Rheotaxis facilitates upstream  
655 navigation of mammalian sperm cells. *Elife* 3, e02403.  
656 <https://doi.org/10.7554/eLife.02403>
- 657 Kim, A.M., Bernhardt, M.L., Kong, B.Y., Ahn, R.W., Vogt, S., Woodruff, T.K.,  
658 O'Halloran, T. V., 2011. Zinc sparks are triggered by fertilization and facilitate cell  
659 cycle resumption in mammalian eggs. *ACS Chem. Biol.* 6, 716–23.  
660 <https://doi.org/10.1021/cb200084y>

- 661 Kirkman-Brown, J.C., Smith, D.J., 2011. Sperm motility: Is viscosity fundamental to  
662 progress? *Mol. Hum. Reprod.* 17, 539–544. <https://doi.org/10.1093/molehr/gar043>
- 663 Kölle, S., Dubielzig, S., Reese, S., Wehrend, A., König, P., Kummer, W., 2009. Ciliary  
664 transport, gamete interaction, and effects of the early embryo in the oviduct: ex vivo  
665 analyses using a new digital videomicroscopic system in the cow. *Biol. Reprod.* 81,  
666 267–274. <https://doi.org/10.1095/biolreprod.108.073874>
- 667 Koyama, H., Shi, D., Fujimori, T., 2019. Biophysics in oviduct: Planar cell polarity, cilia,  
668 epithelial fold and tube morphogenesis, egg dynamics. *Biophys. physicobiology* 16,  
669 89–107. [https://doi.org/10.2142/biophysico.16.0\\_89](https://doi.org/10.2142/biophysico.16.0_89)
- 670 Koyama, H., Shi, D., Suzuki, M., Ueno, N., Uemura, T., Fujimori, T., 2016. Mechanical  
671 Regulation of Three-Dimensional Epithelial Fold Pattern Formation in the Mouse  
672 Oviduct. *Biophys. J.* 111, 650–665. <https://doi.org/10.1016/j.bpj.2016.06.032>
- 673 La Spina, F.A., Molina, L.C.P., Romarowski, A., Vitale, A.M., Falzone, T.L., Krapf, D.,  
674 Hirohashi, N., Buffone, M.G., La Spina, F.A., Puga Molina, L.C., Romarowski, A.,  
675 Vitale, A.M., Falzone, T.L., Krapf, D., Hirohashi, N., Buffone, M.G., 2016. Mouse  
676 sperm begin to undergo acrosomal exocytosis in the upper isthmus of the oviduct.  
677 *Dev. Biol.* 411, 1–11. <https://doi.org/10.1016/j.ydbio.2016.02.006>
- 678 Lewis, S.E., Donnelly, E.T., Sterling, E.S., Kennedy, M.S., Thompson, W., Chakravarthy,  
679 U., 1996. Nitric oxide synthase and nitrite production in human spermatozoa: evidence  
680 that endogenous nitric oxide is beneficial to sperm motility. *Mol. Hum. Reprod.* 2,  
681 873–8.
- 682 Lindemann, C.B., Lesich, K.A., 2016. Functional anatomy of the mammalian sperm  
683 flagellum. *Cytoskeleton* 73, 652–669. <https://doi.org/10.1002/cm.21338>
- 684 Lord Rothschild, F.R.S., 1963. Non-Random Distribution of Bull Spermatozoa in a Drop of  
685 Sperm Suspension. *Nature* 200, 381. <https://doi.org/10.1038/200381b0>
- 686 Miki, K., Clapham, D.E.E., 2013. Rheotaxis guides Mammalian sperm. *Curr. Biol.* 23,  
687 443–52. <https://doi.org/10.1016/j.cub.2013.02.007>
- 688 Miller, M.R., Mannowetz, N., Iavarone, A.T., Safavi, R., Gracheva, E.O., Smith, J.F., Hill,  
689 R.Z., Bautista, D.M., Kirichok, Y., Lishko, P. V., 2016. Unconventional  
690 endocannabinoid signaling governs sperm activation via the sex hormone  
691 progesterone. *Science (80-. )*. 6887, 555–559. <https://doi.org/10.1126/science.aad6887>
- 692 Miraglia, E., Rullo, M.L., Bosia, A., Massobrio, M., Revelli, A., Ghigo, D., 2007.  
693 Stimulation of the nitric oxide/cyclic guanosine monophosphate signaling pathway  
694 elicits human sperm chemotaxis in vitro. *Fertil. Steril.* 87, 1059–1063.  
695 <https://doi.org/10.1016/j.fertnstert.2006.07.1540>
- 696 Moreno-Irusta, A., Dominguez, E.M., Marín-Briggiler, C.I., Matamoros-Volante, A.,  
697 Lucchesi, O., Tomes, C.N., Treviño, C.L., Buffone, M.G., Lascano, R., Losinno, L.,  
698 Giojalas, L.C., 2020. Reactive oxygen species are involved in the signaling of equine  
699 sperm chemotaxis. *Reproduction* 159, 423–436. <https://doi.org/10.1530/REP-19-0480>
- 700 Moreno-Irusta, A., Kembro, J.M., Domínguez, E.M., Matamoros-Volante, A., Gallea,  
701 M.N., Molina, R., Guidobaldi, H.A., Treviño, C.L., Figueras, M.J., Babini, A., Paina,  
702 N.A., Mercado, C.A.N., Giojalas, L.C., 2019. Sperm physiology varies according to

- 703 ultradian and infradian rhythms. *Sci. Rep.* 9, 5988. <https://doi.org/10.1038/s41598->  
704 019-42430-4
- 705 Mortimer, S.T., Mortimer, D., 1990. Kinematics of human spermatozoa incubated under  
706 capacitating conditions. *J. Androl.* 11, 195–203.
- 707 Nosrati, R., Driouchi, A., Yip, C.M., Sinton, D., 2015. Two-dimensional slither swimming  
708 of sperm within a micrometre of a surface. *Nat. Commun.* 6.  
709 <https://doi.org/10.1038/ncomms9703>
- 710 Oliveira, R.G., Tomasi, L., Rovasio, R.A., Giojalas, L.C., 1999. Increased velocity and  
711 induction of chemotactic response in mouse spermatozoa by follicular and oviductal  
712 fluids. *J. Reprod. Fertil.* 115, 23–7.
- 713 Oren-Benaroya, R., Kipnis, J., Eisenbach, M., 2007. Phagocytosis of human post-  
714 capacitated spermatozoa by macrophages. *Hum. Reprod.* 22, 2947–55.  
715 <https://doi.org/10.1093/humrep/dem273>
- 716 Oren-Benaroya, R., Orvieto, R., Gakamsky, A., Pinchasov, M., Eisenbach, M., 2008. The  
717 sperm chemoattractant secreted from human cumulus cells is progesterone. *Hum.*  
718 *Reprod.* 23, 2339–45. <https://doi.org/10.1093/humrep/den265>
- 719 Ounjai, P., Kim, K.D., Lishko, P. V, Downing, K.H., 2012. Three-Dimensional Structure of  
720 the Bovine Sperm Connecting Piece Revealed by Electron Cryotomography1. *Biol.*  
721 *Reprod.* 87, 1–9. <https://doi.org/10.1095/biolreprod.112.101980>
- 722 Pérez-Cerezales, S., Boryshpolets, S., Afanjar, O., Brandis, A., Nevo, R., Kiss, V.,  
723 Eisenbach, M., 2015. Involvement of opsins in mammalian sperm thermotaxis. *Sci.*  
724 *Rep.* 5, 16146. <https://doi.org/10.1038/srep16146>
- 725 Pérez-Cerezales, S., Laguna-Barraza, R., De Castro, A.C., Sánchez-Calabuig, M.J., Cano-  
726 Oliva, E., De Castro-Pita, F.J., Montoro-Buils, L., Pericuesta, E., Fernández-González,  
727 R., Gutiérrez-Adán, A., 2018. Sperm selection by thermotaxis improves ICSI outcome  
728 in mice. *Sci. Rep.* 8, 1–14. <https://doi.org/10.1038/s41598-018-21335-8>
- 729 Que, E.L., Duncan, F.E., Bayer, A.R., Philips, S.J., Roth, E.W., Bleher, R., Gleber, S.C.,  
730 Vogt, S., Woodruff, T.K., O'Halloran, T. V, 2017. Zinc sparks induce physiochemical  
731 changes in the egg zona pellucida that prevent polyspermy. *Integr. Biol. (Camb).* 9,  
732 135–144. <https://doi.org/10.1039/c6ib00212a>
- 733 Ralt, D., Goldenberg, M., Fetterolf, P., Thompson, D., Dor, J., Mashiach, S., Garbers, D.L.,  
734 Eisenbach, M., 1991. Sperm attraction to a follicular factor(s) correlates with human  
735 egg fertilizability. *Proc. Natl. Acad. Sci. U. S. A.* 88, 2840–4.
- 736 Ralt, D., Manor, M., Cohen-Dayag, A., Tur-Kaspa, I., Ben-Shlomo, I., Makler, A., Yuli, I.,  
737 Dor, J., Blumberg, S., Mashiach, S., Eisenbach, M., 1994. Chemotaxis and  
738 chemokinesis of human spermatozoa to follicular factors. *Biol. Reprod.* 50, 774–85.
- 739 Rappa, K., Samargia, J., Sher, M., Pino, J.S., Rodriguez, H.F., Asghar, W., 2018.  
740 Quantitative analysis of sperm rheotaxis using a microfluidic device. *Microfluid.*  
741 *Nanofluidics* 22, 1–11. <https://doi.org/10.1007/s10404-018-2117-6>
- 742 Romero-Aguirregomez-corta, J., Sugrue, E., Martínez-Fresneda, L., Newport, D., Fair, S.,  
743 2018. Hyperactivated stallion spermatozoa fail to exhibit a rheotaxis-like behaviour,  
744 unlike other species. *Sci. Rep.* 8, 1–11. <https://doi.org/10.1038/s41598-018-34973-9>

- 745 Roy, D., Levi, K., Kiss, V., Nevo, R., Eisenbach, M., 2020. Rhodopsin and melanopsin  
746 coexist in mammalian sperm cells and activate different signaling pathways for  
747 thermotaxis. *Sci. Rep.* 10, 1–10. <https://doi.org/10.1038/s41598-019-56846-5>
- 748 Shi, D., Komatsu, K., Hirao, M., Toyooka, Y., Koyama, H., Tissir, F., Goffinet, A.M.,  
749 Uemura, T., Fujimori, T., 2014. *Celsr1* is required for the generation of polarity at  
750 multiple levels of the mouse oviduct. *Dev.* 141, 4558–4568.  
751 <https://doi.org/10.1242/dev.115659>
- 752 Smith, D.J., Gaffney, E.A., Gadelha, H., Kapur, N., Kirkman-Brown, J.C., 2009. Bend  
753 propagation in the flagella of migrating human sperm, and Its modulation by viscosity.  
754 *Cell Motil. Cytoskeleton* 66, 220–236. <https://doi.org/10.1002/cm.20345>
- 755 Spehr, M., Gisselmann, G., Poplawski, A., Riffell, J. a, Wetzel, C.H., Zimmer, R.K., Hatt,  
756 H., 2003. Identification of a testicular odorant receptor mediating human sperm  
757 chemotaxis. *Science* 299, 2054–8. <https://doi.org/10.1126/science.1080376>
- 758 Stewart, C.A., Behringer, R.R., 2012. Mouse oviduct development., in: Kubiak, J.Z. (Ed.),  
759 Results and Problems in Cell Differentiation, Results and Problems in Cell  
760 Differentiation. Springer Berlin Heidelberg, Berlin, Heidelberg, pp. 247–62.  
761 [https://doi.org/10.1007/978-3-642-30406-4\\_14](https://doi.org/10.1007/978-3-642-30406-4_14)
- 762 Su, T., Xue, L., Ozcan, A., 2012. High-throughput lensfree 3D tracking of human sperms  
763 reveals rare statistics of helical trajectories. *Proc. Natl. Acad. Sci. U. S. A.* 109,  
764 16018–22. <https://doi.org/10.1073/pnas.1212506109>
- 765 Su, T.W., Choi, I., Feng, J., Huang, K., McLeod, E., Ozcan, A., 2013. Sperm trajectories  
766 form chiral ribbons. *Sci. Rep.* 3, 1–8. <https://doi.org/10.1038/srep01664>
- 767 Suarez, S.S., 1988. Hamster sperm motility transformation during development of  
768 hyperactivation in vitro and epididymal maturation. *Gamete Res.* 19, 51–65.  
769 <https://doi.org/10.1002/mrd.1120190106>
- 770 Suarez, S.S., Pacey, A.A., 2006. Sperm transport in the female reproductive tract. *Hum.*  
771 *Reprod. Update* 12, 23–37. <https://doi.org/10.1093/humupd/dmi047>
- 772 Sun, F., Bahat, A., Gakamsky, A., Girsh, E., Katz, N., Giojalas, L.C., Tur-kaspa, I.,  
773 Eisenbach, M., 2005. Human sperm chemotaxis: both the oocyte and its surrounding  
774 cumulus cells secrete sperm chemoattractants. *Hum. Reprod.* 20, 761–7.  
775 <https://doi.org/10.1093/humrep/deh657>
- 776 Teves, M.E., Barbano, F., Guidobaldi, H.A., Sanchez, R., Miska, W., Giojalas, L.C., 2006.  
777 Progesterone at the picomolar range is a chemoattractant for mammalian spermatozoa.  
778 *Fertil. Steril.* 86, 745–9. <https://doi.org/10.1016/j.fertnstert.2006.02.080>
- 779 Teves, M.E., Guidobaldi, H.A., Uñates, D.R., Sanchez, R., Miska, W., Giojalas, L.C., 2010.  
780 Progesterone sperm chemoattraction may be modulated by its corticosteroid-binding  
781 globulin carrier protein. *Fertil. Steril.* 93, 2450–2452.  
782 <https://doi.org/10.1016/j.fertnstert.2009.09.012>
- 783 Teves, M.E., Guidobaldi, H.A., Uñates, D.R., Sanchez, R., Miska, W., Publicover, S.J.,  
784 Morales Garcia, A.A., Giojalas, L.C., 2009. Molecular mechanism for human sperm  
785 chemotaxis mediated by progesterone. *PLoS One* 4, e8211.  
786 <https://doi.org/10.1371/journal.pone.0008211>

- 787 Uñates, D.R., Guidobaldi, H.A., Gatica, L.V., Cubilla, M.A., Teves, M.E., Moreno, A.,  
788 Giojalas, L.C., 2014. Versatile action of picomolar gradients of progesterone on  
789 different sperm subpopulations. *PLoS One* 9, e91181.  
790 <https://doi.org/10.1371/journal.pone.0091181>
- 791 Vanderhyden, B.C., Tonary, A.M., 1995. Differential regulation of progesterone and  
792 estradiol production by mouse cumulus and mural granulosa cells by A factor(s)  
793 secreted by the oocyte. *Biol. Reprod.* 53, 1243–50.
- 794 Veitinger, T., Riffell, J.R., Veitinger, S., Nascimento, J.M., Triller, A.,  
795 Chandsawangbhuwana, C., Schwane, K., Geerts, A., Wunder, F., Berns, M.W.,  
796 Neuhaus, E.M., Zimmer, R.K., Spehr, M., Hatt, H., 2011. Chemosensory Ca<sup>2+</sup>  
797 dynamics correlate with diverse behavioral phenotypes in human sperm. *J. Biol.*  
798 *Chem.* 286, 17311–25. <https://doi.org/10.1074/jbc.M110.211524>
- 799 Wang, S., Burton, J.C., Behringer, R.R., Larina, I. V., 2015. In vivo micro-scale  
800 tomography of ciliary behavior in the mammalian oviduct. *Sci. Rep.* 5, 1–11.  
801 <https://doi.org/10.1038/srep13216>
- 802 Wang, S., Larina, I. V., 2018a. In vivo three-dimensional tracking of sperm behaviors in the  
803 mouse oviduct. *Development* 145, dev157685. <https://doi.org/10.1242/dev.157685>
- 804 Wang, S., Larina, I. V., 2018b. In vivo imaging of the mouse reproductive organs, embryo  
805 transfer, and oviduct cilia dynamics using optical coherence tomography. *Methods*  
806 *Mol. Biol.* 1752, 53–62. [https://doi.org/10.1007/978-1-4939-7714-7\\_5](https://doi.org/10.1007/978-1-4939-7714-7_5)
- 807 Yanagimachi, R., 1970. The movement of golden hamster spermatozoa before and after  
808 capacitation. *J. Reprod. Fertil.* 23, 193–6. <https://doi.org/10.1530/jrf.0.0230193>
- 809 Yániz, J.L., Carretero, T., Recreo, P., Arceiz, E., Santolaria, P., 2014. Three-dimensional  
810 architecture of the ovine oviductal mucosa. *J. Vet. Med. Ser. C Anat. Histol. Embryol.*  
811 43, 331–340. <https://doi.org/10.1111/ahe.12078>
- 812 Yániz, J.L., Lopez-Gatius, F., Hunter, R.H.F., 2006. Scanning electron microscopic study  
813 of the functional anatomy of the porcine oviductal mucosa. *Anat. Histol. Embryol.* 35,  
814 28–34. <https://doi.org/10.1111/j.1439-0264.2005.00634.x>
- 815 Yániz, J.L., Lopez-Gatius, F., Santolaria, P., Mullins, K.J., 2000. Study of the functional  
816 anatomy of bovine oviductal mucosa. *Anat. Rec.* 260, 268–78.
- 817 Zaferani, M., Cheong, S.H., Abbaspourrad, A., 2018. Rheotaxis-based separation of sperm  
818 with progressive motility using a microfluidic corral system. *Proc. Natl. Acad. Sci. U.*  
819 *S. A.* 115, 8272–8277. <https://doi.org/10.1073/pnas.1800819115>
- 820 Zamir, N., Riven-Kreitman, R., Manor, M., Makler, A., Blumberg, S., Ralt, D., Eisenbach,  
821 M., 1993. Atrial natriuretic peptide attracts human spermatozoa in vitro. *Biochem.*  
822 *Biophys. Res. Commun.* 197, 116–22. <https://doi.org/10.1006/bbrc.1993.2449>
- 823 Zhang, Z., Liu, J., Meriano, J., Ru, C., Xie, S., Luo, J., Sun, Y., 2016. Human sperm  
824 rheotaxis: A passive physical process. *Sci. Rep.* 6, 1–8.  
825 <https://doi.org/10.1038/srep23553>

827 **Legends for figures**

828 **Fig. 1. Anatomy of the oviduct regions. (A)** Transversal and the corresponding  
829 longitudinal representations of the isthmus, isthmus-ampulla junction (IAJ), and  
830 ampulla regions are shown. An oocyte is drawn to scale inside the ampulla cross-  
831 section. **(B)** A three-dimensional representation of the lumen of the oviduct  
832 corresponding to the three regions shown in A. IAJ, isthmus-ampulla junction.  
833 (Figure adapted from Yániz et al., 2000; 2014).

834

835 **Fig. 2. Factors affecting oviduct fluid movement.** All images are schematic  
836 representations of the isthmus, the isthmus-ampulla junction (IAJ), and the  
837 ampulla. **(A)** Secretion of oviduct fluid by the secretory epithelial cells,  
838 represented by vertical arrows, which are of different sizes to show that the  
839 amount of fluid is high in the isthmus and gradually diminishes towards the  
840 ampulla. The dotted line ending in an arrow at the right, represents the  
841 direction of the fluid flow. **(B)** Cilia from ciliated cells, present in the oviduct  
842 epithelium, beat in the direction of the uterus. Dotted lines and arrows  
843 represent the direction of the fluid movement along the lumen between folds.  
844 The red lines indicate the position of cilia responsible for forming the fluid flow.  
845 **(C)** The wave of peristalsis is shown along the oviduct. The drops of fluid are  
846 represented in the lumen of the tube. In the lower isthmus, the drops move  
847 equally back and forward, in the middle they move mainly forward, and in the  
848 ampulla they continue moving ahead (see the direction of the arrows in each  
849 drop). The arrow to the right of the tube shows the direction of the oviduct fluid  
850 flow.

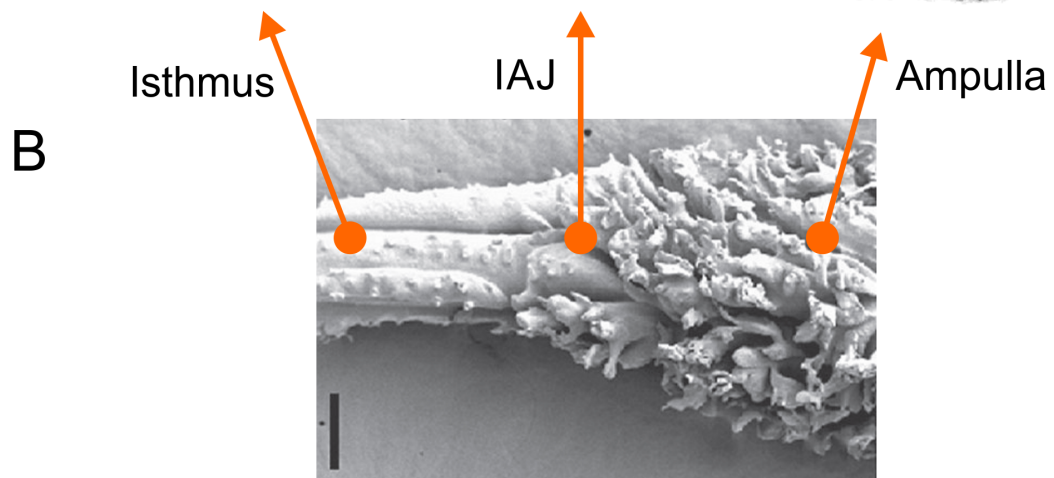
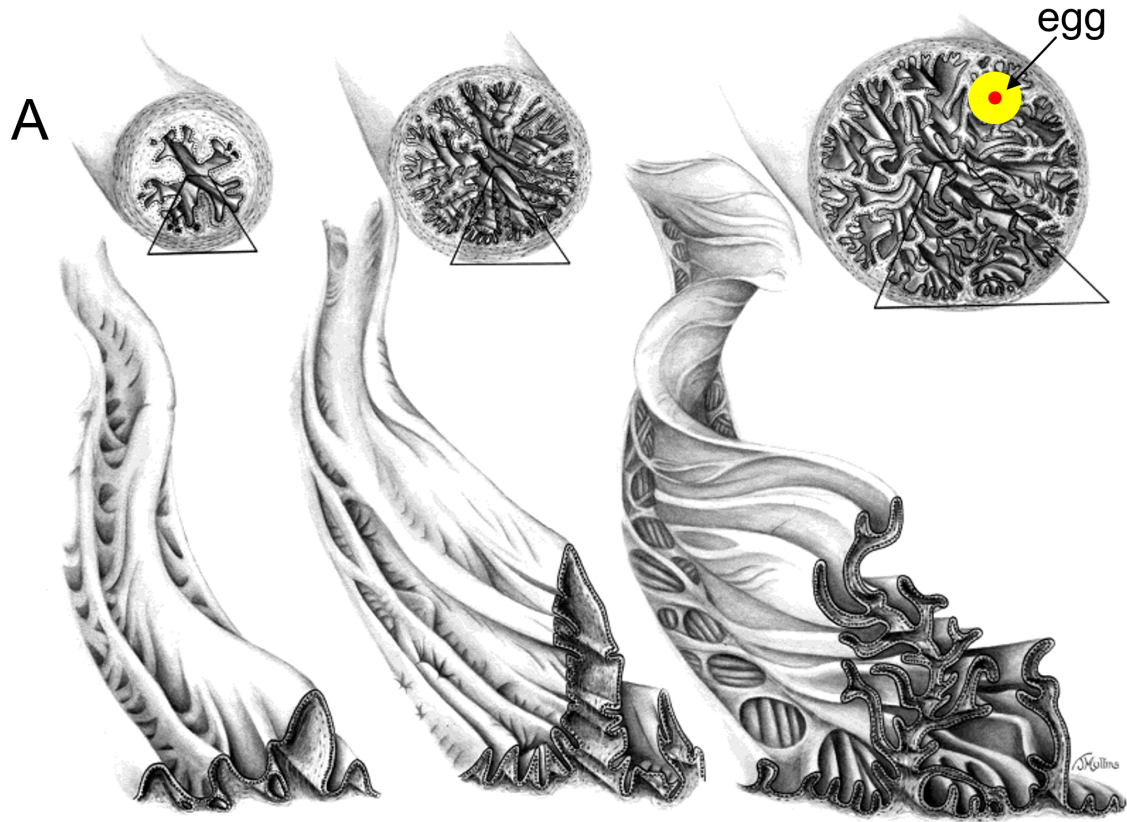
851

852 **Fig. 3. Representation of sperm taxis.** The position of the spermatozoa show the  
853 direction they are swimming. In the case of rheotaxis **(A)**, the spermatozoa are  
854 aligned against the fluid flow, which is represented with an arrow pointing its  
855 direction. In thermotaxis **(B)**, spermatozoa orient themselves by following a  
856 temperature gradient, swimming from the cooler to the warmer place. In  
857 chemotaxis **(C)**, spermatozoa are guided by following a concentration gradient  
858 of an attractant substance, swimming in the direction of its source. In  
859 chemorepulsion **(D)**, spermatozoa swim against the source of the substance  
860 down its concentration gradient.

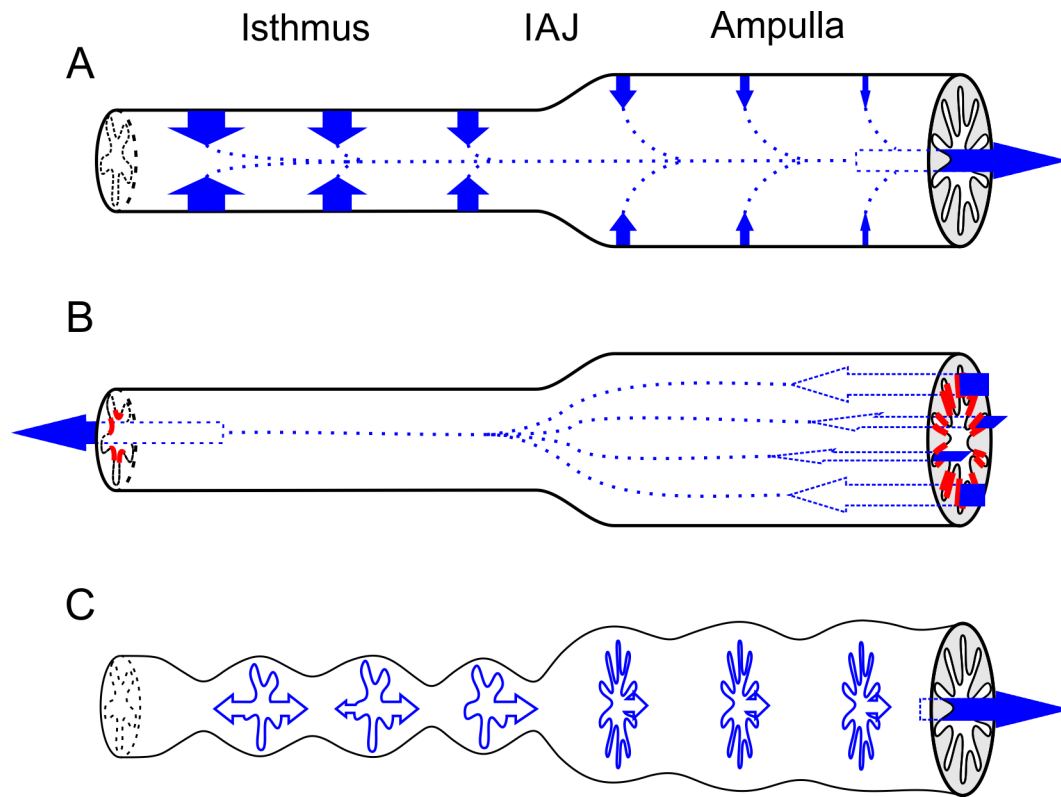
861

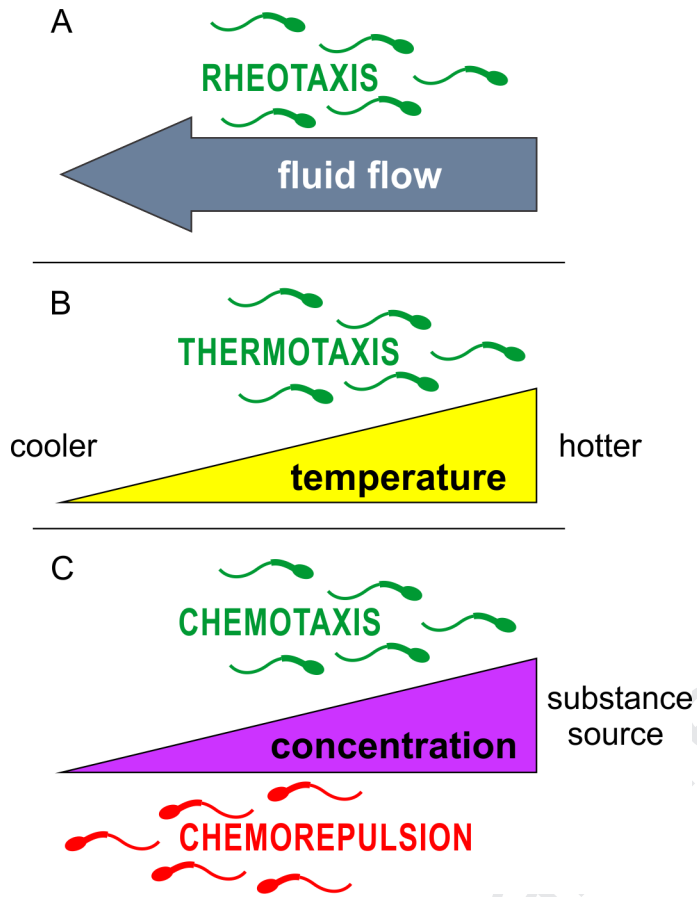
862 **Fig. 4. A theoretical model to explain sperm getting to and away from the**  
863 **oocyte.** See the explanation in the text.

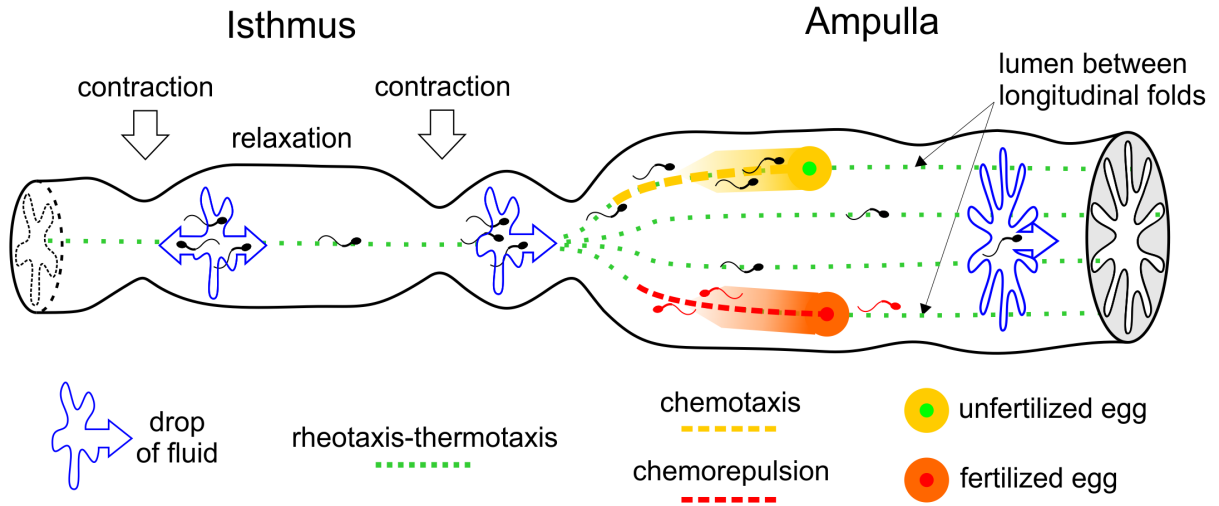
864











Journal Pre-proof